The Journal of Immunology

RESEARCH ARTICLE | FEBRUARY 01 2020

cDC1 IL-27p28 Production Predicts Vaccine-Elicited CD8+ T Cell Memory and Protective Immunity

Augustus M. Kilgore; ... et. al

J Immunol (2020) 204 (3): 510–517.
https://doi.org/10.4049/jimmunol.1901357

cDC1 IL-27p28 Production Predicts Vaccine-Elicited CD8$^+$ T Cell Memory and Protective Immunity

Augustus M. Kilgore,* Nathan D. Pennock,† and Ross M. Kedl*

Although adjuvants and formulations are often either empirically derived, or at best judged by their ability to elicit broad inflammation, it would be ideal if specific innate correlates of adaptive immunity could be identified to set a universally applicable benchmark for adjuvant evaluation. Using an IL-27 reporter transgenic mouse model, we show in this study that conventional type 1 dendritic cell IL-27 production in the draining lymph node 12 h after s.c. vaccination directly correlates with downstream CD8$^+$ T cell memory and protective immunity against infectious challenge. This correlation is robust, reproducible, predictive, entirely unique to vaccine biology, and is the only innate correlate of CD8$^+$ T cell immune memory yet to be identified. Our results provide new insights into the basic biology of adjuvant-elicited cellular immunity and have clear implications for the screening and evaluation of novel adjuvants. ***The Journal of Immunology*****, 2020, 204: 510–517.**

Over the past several decades, our understanding of CD8 T cell biology and the formation of protective cellular-mediated immune memory has expanded greatly, driven significantly by robust murine models of infection, such as *Listeria monocytogenes* and lymphocytic choriomeningitis virus (1, 2). These models have facilitated insights into how CD8 T cells encounter Ag, become activated, expand, and contract over time to form stable protective memory pools. It is reasonable to assume that the "rules" of T cell behavior established in these systems may be applied toward understanding an immune response against an unknown infectious agent. Their applicability to subunit vaccination has become more questionable. Indeed, a growing body of research now suggests that key elements of our understanding of T cell biology derived from infectious models do not apply to subunit vaccine-elicited cellular immunity, and vice versa. For example, there is an obligate role for IL-27 (3, 4) and IL-15 (4) in facilitating maximal vaccine-elicited CD4 and CD8$^+$ T cell responses to the majority of vaccine adjuvants, whereas the loss of either of these cytokines does not diminish the CD4 or CD8 T cell responses against infectious challenge (3, 5–8).

Not only does the biology of vaccine-elicited cellular immunity appear to diverge from that of infectious biology, it also seems to diverge from that of historical vaccinology. A good example of this is the role of the Ag "depot" in establishing protective humoral immunity. Achieved through the formulation of the Ag in an emulsion or precipitate, the depot slowly releases Ag and inflammation from the injection site and into the draining secondary lymphoid tissues. Although an Ag depot has long been known to be unnecessary for achieving protective humoral immunity (9), it is clear that exposure of draining lymphoid tissue to Ag over many weeks does enhance the magnitude and affinity of neutralizing Ab (10–14). However, it is also equally clear that that the use of tissue-persisting Ag depots does irreparable damage to the formation of T cell memory and subsequent protective immunity (15–17). Thus, a better understanding of vaccine-elicited T cell immunity cannot always borrow from the historical rules of classic vaccinology.

Given the central role for IL-27 in mediating the T cell response to subunit vaccination, we explored the hypothesis that IL-27 might be an innate correlate of vaccine-elicited T cell immunity. Specifically, we sought to determine whether the amount of IL-27 induced by a specific adjuvant, within the lymphoid tissue draining a peripheral injection site, was predictive of the ensuing T cell response. IL-27 is a pleotropic cytokine of the IL-12 family (18), comprised of a heterodimer of EBI3 and p28 (19). As p28 is the more dynamically regulated subcomponent, we generated a construct containing enhanced GFP (eGFP) downstream of ∼7 kb of the p28 locus 5′ to the transcriptional start site (20). This transgene was used to produce a mouse (IL-27p28-eGFP) in which the GFP faithfully reports IL-27p28 expression within various APC subsets (20).

Using this IL-27p28-eGFP, we show in this study that p28-eGFP is induced in draining lymph node (LN) conventional type 1 dendritic cells (DCs) (cDC1s) in response to a variety of adjuvants. The amount of p28-eGFP induced by each adjuvant at 12 h after s.c. vaccination successfully predicted the magnitude of Ag-specific CD8 memory precursor effector cells (MPECs) as well as the magnitude of durable CD8$^+$ T cell memory and its capacity for host protection. The strength of this correlation was such that the p28-eGFP expression could even be used to accurately predict the magnitude of the T cell response to previously untested adjuvants, indicating its potential for adjuvant screening efforts. To the best of our knowledge, this is the only instance in which a memory CD8$^+$ T cell response can be predicted and stratified by a single innate factor produced as early as 12 h after vaccination. Adjuvants that induce more sustained inflammation, like CpG, increased the overall frequency of Ag-specific CD8$^+$

*Department of Immunology and Microbiology, University of Colorado Anschutz Medical Campus, Aurora, CO 80045; and †Oregon Health and Science University, Portland, OR 97239

ORCIDs: 0000-0001-5374-7843 (N.D.P.); 0000-0002-9065-7895 (R.M.K.).

Received for publication November 13, 2019. Accepted for publication November 23, 2019.

This work was supported by National Institutes of Health Grants AI066121, AI117918, and AI12689.

Address correspondence and reprint requests to Dr. Ross M. Kedl, University of Colorado Anschutz Medical Campus, Mail Stop 8333, Room P18-8115, 12800 E. 19th Avenue, Aurora, CO 80045-2537. E-mail address: ross.kedl@cuanschutz.edu

The online version of this article contains supplemental material.

Abbreviations used in this article: DC, dendritic cell; dPLN, draining popliteal LN; eGFP, enhanced GFP; gMFI, geometric mean fluorescence intensity; LM-OVA, OVA-expressing *Listeria monocytogenes*; LN, lymph node; MPEC, memory precursor effector cell; MPL, monophosphoryl lipid A; polyIC, polyinosinic-polycytidylic acid; SLEC, short-lived effector cell.

T cells through the generation of short-lived effector cells (SLECs) without affecting the predictive capacity of the p28-eGFP/MPEC correlation. These data suggest that the frequency of memory precursors is dictated very early after vaccination and that ongoing inflammation helps form terminal effectors without diversion from the memory precursor pool.

Materials and Methods

Mice

C57BL/6 mice were obtained from The Jackson Laboratory or produced in our own facility. IL-27p28-eGFP mice (20) were produced and maintained in our own facility at the University of Colorado Anschutz Medical Campus. CCR7-GFP mice (C57BL/6-*Ccr7*$^{tm1.1Dmc}$/J) were obtained from The Jackson Laboratory and bred in our facility to C57BL/6 to obtain heterozygous CCR7-GFP reporter mice. All experiments were conducted in accordance with protocols approved by the University of Colorado Denver Institutional Animal Care and Use Committee.

Immunization and infection

For footpad immunization, mice were anesthetized with isoflurane, after which 20–25 μg of detoxified whole chicken OVA (Sigma) or OVA Alexa Fluor 647 conjugate (Thermo Fisher Scientific) combined with 0.002–20 μg polyinosinic-polycytidylic acid (polyIC; GE Healthcare) or 10 μg lipoteichoic acid (InvivoGen), monophosphoryl lipid A (MPL; InvivoGen), CpG (InvivoGen), 3M-012, Pam3Cys (InvivoGen), flagellin (InvivoGen), or α-Gal-Cer (Enzo Life Sciences) or a 1/10 dilution of Adjuplex (21) in a total volume of 30–40 μl PBS was administered s.c. in the hind footpad of the mouse. For i.m. immunization, 20 μg OVA combined with 10 μg of polyIC in a total volume of 40 μl PBS was administered to the quadriceps of anesthetized mice. For ear immunization, 20 μg OVA combined with 10 μg of polyIC in a total volume of 20 μl PBS was administered between the layers of the ear of anesthetized mice. For experiments in which multiple time points were examined, immunizations were administered such that all harvests occurred simultaneously. For OVA-expressing *Listeria monocytogenes* (LM-OVA) protection assays, mice that had received footpad immunizations as above 50–80 d prior received 100,000 CFU of erythromycin-resistant LM-OVA via tail vein injections. At time of infectious challenge, mice were bled via the tail vein to examine resting-state levels of memory T cells. Four days after challenge, livers and spleens were harvested, weighed, homogenized, and subjected to cell lysis, and the resulting slurry was plated in serial dilution on brain–heart infusion agar plates containing 5 μg/ml erythromycin. After 36 h of incubation at 37°C, the plates were removed, and the resulting colonies were quantified.

Isolation of cells

For isolation of dendritic and other innate immune cells from draining LN, footpad immunized mice were first euthanized by CO_2 at the indicated time points. The draining popliteal LN (dPLN) was then removed and minced with tweezers in 1 ml Click's Medium (FUJIFILM Irvine Scientific) containing 1 mg/ml Collagenase D (Roche) and 50 μg/ml DNase I (Worthington Biochemical) per LN. After a 45-min incubation at 37°C, 1 ml 0.1 M EDTA was added, and cells were allowed to incubate another 5 min. Disassociated cells were then washed with HBSS (Life Technologies) containing 5 mM EDTA and forced through 100-μm strainers to generate single cell suspensions. For isolation of T cells from the spleen and LNs of immunized mice, organs were harvested at indicated time points and forced through 100-μm strainers to generate single cell suspensions. In the case of T cells, cell suspensions were counted on a Vi-CELL automated cell counter (Beckman Coulter) to determine total viable cell number. To quantify innate cells, the entire sample, representing the entire LN, was collected during flow cytometry analysis.

Flow cytometry

Kb-SIINFEKL tetramer was provided by the National Institutes of Health tetramer core. For Ab staining, the following Abs were used: anti-CD64 (X54-5/7.1), anti–MHC class II (M5/114.15.2), BV421 anti-mouse Ly6C (HK1.4; BioLegend), BV510 anti-mouse Ly6G (1A8; BioLegend), anti-CD44 (IM7), anti-CD11c (N418), anti-XCR1 (ZET), anti-CD8 (53-6.7), anti-KLRG1 (2F1/KLRG1), and anti-CD103 (2E7) from BioLegend; and anti-CD62L (MEL-14), anti-CD3 (17A2), anti-B220 (RA3-6B2), anti-CD19 (1D3), anti-CD11b (M1/70) and anti-CD127 (A7R34) from Tonbo Biosciences. Samples were collected on a CytoFlex S (Beckman Coulter), and analysis was performed using FlowJo software (version 10.5.3). Specific cell populations were gated on follows: T cells: Live, B220$^-$, CD11c$^-$, and CD3$^+$; B cells: Live, B220$^+$, CD11c$^-$, and CD3$^-$; cDC1: CD3/B220$^-$, CD11c$^+$, and XCR1$^+$; cDC2: CD3/B220$^-$,CD11c$^+$, CD11b$^+$, and XCR1$^-$; and monocytes: CD64$^+$, CD11b^{hi}, Ly6C^{hi}, and Ly6G^{lo}.

Statistics

Prism (v8; GraphPad) was used to perform all statistical analysis. One-way ANOVAs with multiple comparisons were used to identify adjuvants that had a significantly different effect on the measured outcome relative to other adjuvants. Unpaired Student *t* tests were used to identify differences between individual groups. Experiments were performed two or more times each, with three or more mice per group. Where data are correlated with other data, correlations were checked against repeats. Data indicate means ± SEM unless otherwise noted.

Results

cDC1 DCs are the primary producers of IL-27p28 following immunization

We previously published on the use of an IL-27p28-eGFP reporter mouse in which a GFP signal indicates the presence and amount of p28 expression (20). Those experiments not only validated the concurrence of the reporter with IL-27p28, but also identified 1) cDC1s and monocytes as the primary producers of IL-27p28 in the spleen after i.v. adjuvant administration and 2) a direct correlation between cDC1 reporter expression at 4 h with CD8$^+$ T cell expansion at 7 d in the spleen post-i.v. immunization (20). Because the route of immunization can influence the activation of innate immunity and the subsequent magnitude, duration, and localization of the T cell response to immunization, we examined the p28-eGFP reporter expression in APC subsets within the draining LN after various forms of local vaccine administration. To minimize any potentially confounding influences of the Ag (tissue retention/bioavailability, lymphatic draining, Ag uptake, class I binding, etc.), we used the model Ag OVA, for which numerous cellular and molecular tools are available for dissecting immune response parameters and mechanisms. Initially, mice were immunized s.c. in the footpad with OVA and polyIC. At 12 h after immunization, the dPLN were harvested, digested into a single cell suspension, and the p28-eGFP reporter expression determined in T cells, B cells, cDC1 (CD3/B220$^-$, CD11c$^+$, XCR1$^+$), cDC2 (CD3/B220$^-$, CD11c$^+$, CD11b$^+$, XCR1$^-$), and monocytes (CD64$^+$, CD11b^{hi}, Ly6C^{hi}, Ly6G^{lo}) by flow cytometry. Consistent with previous reports (20, 22, 23), cDC1s were the primary producers of IL-27p28 (Fig. 1A, 1B), with 40–70% of cDC1s in the dPLN p28-eGFP$^+$ following immunization. cDC2s and monocytes also expressed the p28-eGFP reporter (Fig. 1B), although at significantly lower frequencies than cDC1s. Based on a correlation we previously established between IL-27p28 message and the p28-eGFP reporter geometric mean fluorescence intensity (gMFI), we noted that cDC1s also produce substantially more IL-27p28 on a per cell basis (Fig. 1C). cDC1s also produced IL-27p28 within draining LNs after either intradermal (ear) or i.m. immunization (Fig. 1D, 1E), indicating that this was not a phenomenon exclusively associated with the footpad/dPLN.

Given the short lifespan of DCs (24, 25) and the corresponding narrow window for T cell activation, we next examined the timing of cDC1 activation, Ag uptake, and p28-eGFP reporter expression in the dPLN following footpad immunization. Initially, B6 mice were immunized with polyIC, dPLNs were harvested at various points following immunization, and the relative frequencies of cDC1 and cDC2 were analyzed. We observed two peaks in overall DC numbers, at 12 and 24 h. In both frequency (Fig. 2A) and total numbers (Fig. 2B), representation of the two DC subsets shifted from predominantly cDC2s at 0 h to majority cDC1s at 12 h to being split between cDC1s and cDC2s by 24 h. Over this time, DCs also increased in class II expression (Fig. 2A) and in number

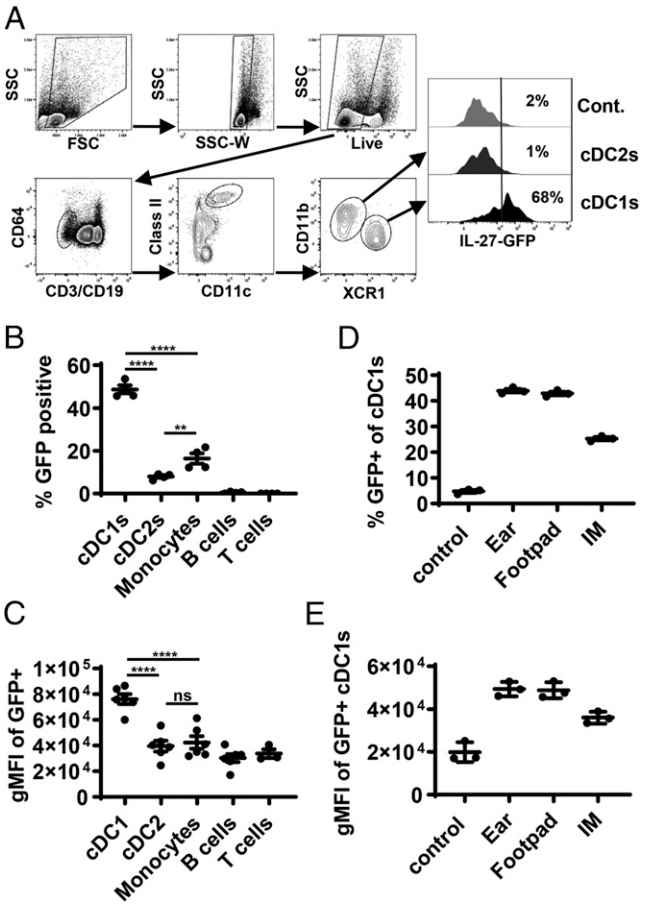

FIGURE 1. IL-27p28 is made by cDC1s in the draining node following peripheral subunit immunization. (**A**–**E**) IL-27p28-eGFP mice were immunized in the footpad (A–C) or footpad, ear, or thigh muscle (D and E) with 10 μg polyIC and 25 μg OVA, and draining LNs were harvested 6–12 h later. (A) Representative gating strategy identifying cDC1s and demonstrating GFP signal following immunization. (B and C) cDC1s, cDC2s, monocytes, B cells, and T cells were identified to determine IL-27p28-eGFP production by each cell type. (D and E) The GFP signal from cDC1s was measured in the cervical, popliteal, and inguinal draining LNs following immunization between the ear layers, in the footpad, or in the thigh, respectively. Data indicate means ± SEM, $n \geq 3$ mice per group, representative of two or more experiments. $^{**}p < 0.01$, $^{****}p < 0.0001$.

(Fig. 2B), consistent with their activation and accumulation. DC accumulation within the node can occur through the proliferation of DC precursors (24–26) and the accumulation of migratory DCs (27, 28). As previous studies have shown numbers of migratory DCs peaking at ~24 h (29), our data suggested the possibility of an early (12 h) peak in resident DC expansion/frequency and a subsequent (24 h) peak in migratory DCs. We confirmed this hypothesis using heterozygous CCR7-GFP knock-in reporter mouse, in which essentially all DCs harvested at 12 h after immunization were resident ($CCR7^{low}$) (Fig. 2C, 2D), whereas by 24 h, the DC pool was split between resident and migratory ($CCR7^{high}$) DCs, with a decline in the number of resident cDC1s (Fig. 2C, 2D). However, total (resident and migratory) cDC1 frequency and numbers were generally highest at 12 h after immunization (Fig. 2E, 2F). Using the p28-eGFP reporter host to assess IL-27p28 production, we observed that the number of IL-27p28 producing cDC1s was also highest at 12 h (Fig. 2G). The gMFI of the p28-eGFP did not change substantially in cDC1s between 12 and 24 h (Fig. 2H), indicating that the amount of IL-27p28 produced on a per cell basis is not substantially different between migratory and resident cDC1s. Together, these results indicate that following peripheral immunization, 1) both resident and migratory cDC1s are the primary producers of IL-27p28 in the draining node, 2) the number of IL-27p28–producing cDC1s peaks at 12 h after immunization, and 3) this peak consists primarily of resident cDC1s.

Early LN IL-27p28 predicts the frequency of circulating Ag-specific T cells

We next examined the cDC1 response at 12 and 24 h after footpad immunization to a range of adjuvants. At 12 h, polyIC had the greatest impact on the percentage of p28-$eGFP^+$ cDC1s (Fig. 3A), the total number of p28-$eGFP^+$ cDC1s (Fig. 3B), and cDC1 p28-eGFP gMFI (Fig. 3C). PolyIC cDC1s continued to show the highest percentage of p28-$eGFP^+$ and p28-eGFP gMFI at 24 h (Fig. 3A, 3C), but by this time point, CpG was the greatest in regard to total cellularity (Supplemental Fig. 1A), total DCs (Supplemental Fig. 1B), total cDC1s (Supplemental Fig. 1C), and p28-$eGFP^+$cDC1s (Fig. 3B), with polyIC matched in all these values by the TLR7 agonist 3M-012.

We next established the magnitude of the CD8 T cell response generated by each adjuvant. At 7 d following footpad immunization, dPLNs, blood, and spleens were harvested, and the magnitude of the T cell response was examined by tetramer staining (Fig. 3D). CpG produced by far the largest T cell response within the dPLN, followed by all others at a much lower level (Fig. 3D, 3E). In contrast to the response in the node, a different hierarchy of adjuvant efficacy was seen in the number of circulating Ag-specific T cells in the spleen, in which polyIC produced the greatest response, followed by MPL and then the remaining adjuvants (Fig. 3D, 3E, lower panels). This hierarchy also held true for the blood (Supplemental Fig. 1D), indicating that the number of Ag-specific T cells still in the draining node 7 d after subunit immunization does not correlate with the number of circulating adjuvant-elicited T cells (Supplemental Fig. 1E). This divergence in dPLN versus systemic T cell numbers tracks somewhat with differences in sustained draining node inflammation (as measured by DC and total LN cellularity) (Supplemental Fig. 1A, 1B) and suggests that the numbers of T cells in the draining LN late after immunization may better reflect the LN retention of T cells than the efficacy of their generation.

We next assessed whether any particular cDC1 parameter from the dPLN was predictive of the splenic CD8 T cell response. We compared the various early response metrics described above with the corresponding number of T cells in the spleen resulting from each adjuvant. We found that total cDC1 numbers (Supplemental Fig. 2A, 2B) and even p28-eGFP cDC1 numbers (Supplemental Fig. 2C, 2D) at 12 or 24 h after immunization were not predictive of T cell numbers 7 d later. In contrast, we found a strong correlation between the cDC1 p28-eGFP gMFI in the draining node at 12 h and T cell numbers in the spleen but not the dPLN (Fig. 3F). In keeping with our previous data (20), this correlation held best with the p28-eGFP gMFI but not the number of cells producing IL-27p28. The strength and significance of this correlation held even when eliminating polyIC from consideration (Supplemental Fig. 2E), indicating that the values associated with the polyIC response are not unduly influencing the predictive value of the 12 h p28-eGFP gMFI signal. Interestingly, the significance of the correlation between T cell response and p28-eGFP gMFI did not hold for the cDC1s at 24 h (Supplemental Fig. 2F).

IL-27p28 predicts adjuvant-elicited $CD8^+$ T cell memory precursors and long-term memory

Ultimately, the goal of vaccination is the generation of a stable pool of protective memory cells. This pool is heavily influenced by the

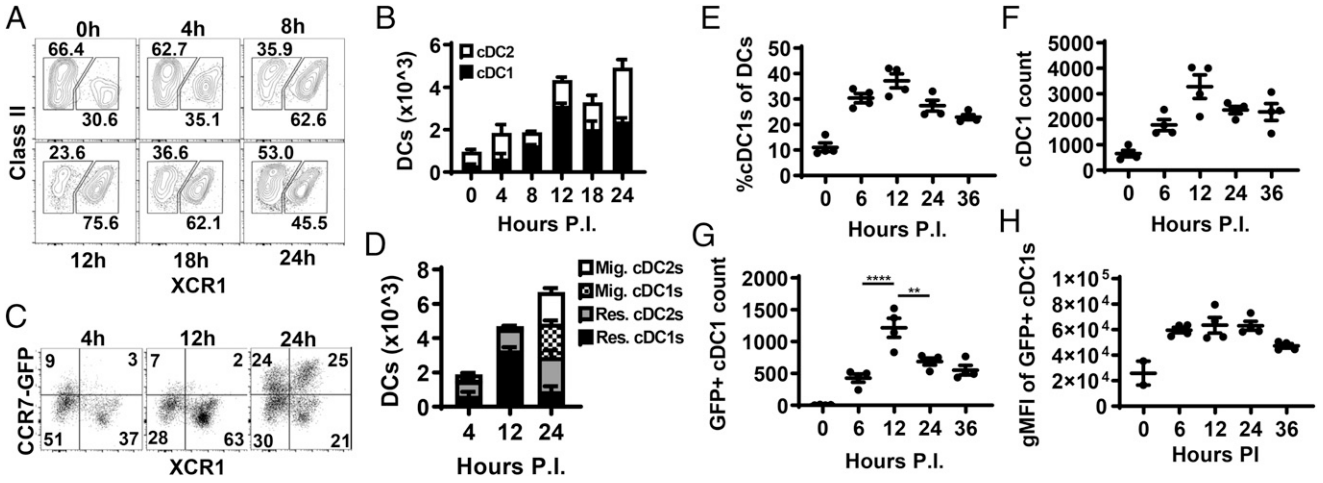

FIGURE 2. cDC1 IL-27p28 production in the dPLN peaks at 12 h after immunization. (**A**–**H**) C57BL/6 (A and B), C57BL/6-*Ccr7*$^{tm1.1Dnc}$/J (C and D), or IL-27p28-eGFP (E–H) mice were immunized in the footpad with 10 μg polyIC and 25 μg OVA, and dPLNs were harvested and examined by flow cytometry at the indicated time point. (A and B) Gated on total DCs. (C–H) Gated on total DCs or as indicated. Data indicate means ± SEM, $n \geq 3$ mice per group, representative of two or more experiments. $^{**}p < 0.01$, $^{****}p < 0.0001$.

peak magnitude of the primary response, a time point that can vary across different adjuvants for a variety of reasons. Indeed, although the peak response to adjuvants such as polyIC and MPL are established at 7 d after immunization, the response to CpG often peaks between day 7 and 10 (Supplemental Fig. 3A). In quantifying the total T cell response at this later time point, we observed a loss of correlation with the 12-h LN cDC1 p28-eGFP gMFI (Supplemental Fig. 3B), the result of an expansion of CD127^{lo}KLRG$^{+/-}$ T cells (Fig. 4A, 4B). However, the predictive power of the p28-eGFP gMFI held with respect to the number of MPEC T cells generated by each adjuvant (Fig. 4C). The number of SLECs and MPECs did not correlate with one another (Supplemental Fig. 3C), with CpG appearing to drive a large expansion of SLECs with minimal impact to the MPEC pool (Fig. 4B).

To determine if the trend in MPEC numbers was related to memory, we next examined the T cell memory pool at 80 d after immunization and its correlation with 12-h LN IL-27p28 production. Mice immunized with adjuvants that gave rise to large pools of SLECs at early time points also contained relatively large reservoirs of effector-like (KLRG1$^+$, CD127$^-$) cells at memory time points (Fig. 4D). This meant that, as with 10 d following immunization, IL-27p28 production at 12 h was not predictive of the total frequency of Ag-specific T cells at these late time points (Supplemental Fig. 3D). However, 12-h cDC1 p28-eGFP gMFI continued to be highly predictive of the pool of KLRG$^-$ and CD127$^+$ cells (Fig. 4E). Given the demonstrated protective capacity of CD127^{hi} T cells (30), we predicted that the frequency of these memory cells after immunization would also correlate with protection against subsequent infection. To this end, we challenged memory-stage mice with LM-OVA and measured the bacterial load in the liver after 4 d as an indicator of CD8$^+$ T cell–mediated host protection. As predicted, we found a strong correlation between the frequency of CD127^{hi} cells and control of infection 80 d later (Fig. 4E, 4F). Because of the association between early IL-27p28 and memory cell frequency (Fig. 4E), this meant that IL-27p28 production at 12 h after immunization successfully predicted T cell–mediated host protection 80 d later (Fig. 4G).

As noted previously, the strength of the IL-27p28/T cell correlation was not simply due to the signal derived from the response to polyIC as a statistically significant correlation was maintained even after eliminating polyIC from consideration (Supplemental Figs. 2E, 3E). To ensure that our correlation was not coincidental with the amount of adjuvant used, we immunized mice with a dose titration of polyIC and again tracked 12-h cDC1 p28-eGFP gMFI and T cell generation. Using 10-fold titrations, we observed a peak of p28-eGFP gMFI at 2 μg of polyIC injected into the footpad, which consistently declined slightly at 20 μg (Fig. 5A), a common characteristic of the response to innate receptor agonists (31). As predicted by our previous data, the magnitude of the CD8 T cell response (Fig. 5B) continued to correlate with the amount of IL-27p28 produced by cDC1s at 12 h (Fig. 5C).

As the data overwhelmingly supports a predictive relationship between IL-27p28 and CD8$^+$ T cell MPEC and memory formation, we next used the existing model to predict the T cell response to untested adjuvants. We selected two adjuvants, the TLR5 agonist flagellin (32) and the CD1-binding NKT cell stimulus αGalCer (33) and measured the p28-eGFP gMFI of p28-producing cDC1s 12 h after footpad immunization (Fig. 5D). Using the polyIC-induced cDC1 GFP gMFI in this experiment, we normalized the p28-eGFP gMFI values for each adjuvant to the mean polyIC p28-eGFP gMFI in the experiment from Fig. 4C. We then used the associated line equation (in which y is the normalized gMFI and x is the T cell value) to obtain a predicted range of MPECs for each adjuvant (Fig. 5E, shaded boxes). This predicted range fit well within the SD of the actual number of MPECs, obtained from B6 mice immunized concomitant with the p28-eGFP mice and analyzed 10 d after immunization (Fig. 5E, closed circles). When overlaid onto the correlation from Fig. 4C, the error of the observed values fell within the previously generated linear regression, indicating a high level of predictability (Fig. 5F). Thus, IL-27p28 production from cDC1s at 12 h accurately predicts the efficacy by which an adjuvant will generate CD8 T cell memory.

Discussion

Previously, we published that following systemic immunization, IL-27 production in the splenic cDC1 subset could predict the magnitude of the bulk T cell response at 7 d (20). Missing from this previous data, however, were the use of a route more appropriate to typical vaccinations or any correlates to long-term memory responses. The present data address these important issues in vaccine biology, using the p28-eGFP reporter to stratify commonly used vaccine adjuvants and predict consequent memory T cell frequency and protective capacity. Although IL-27's influence on T cell memory has been noted, the literature is contradictory as

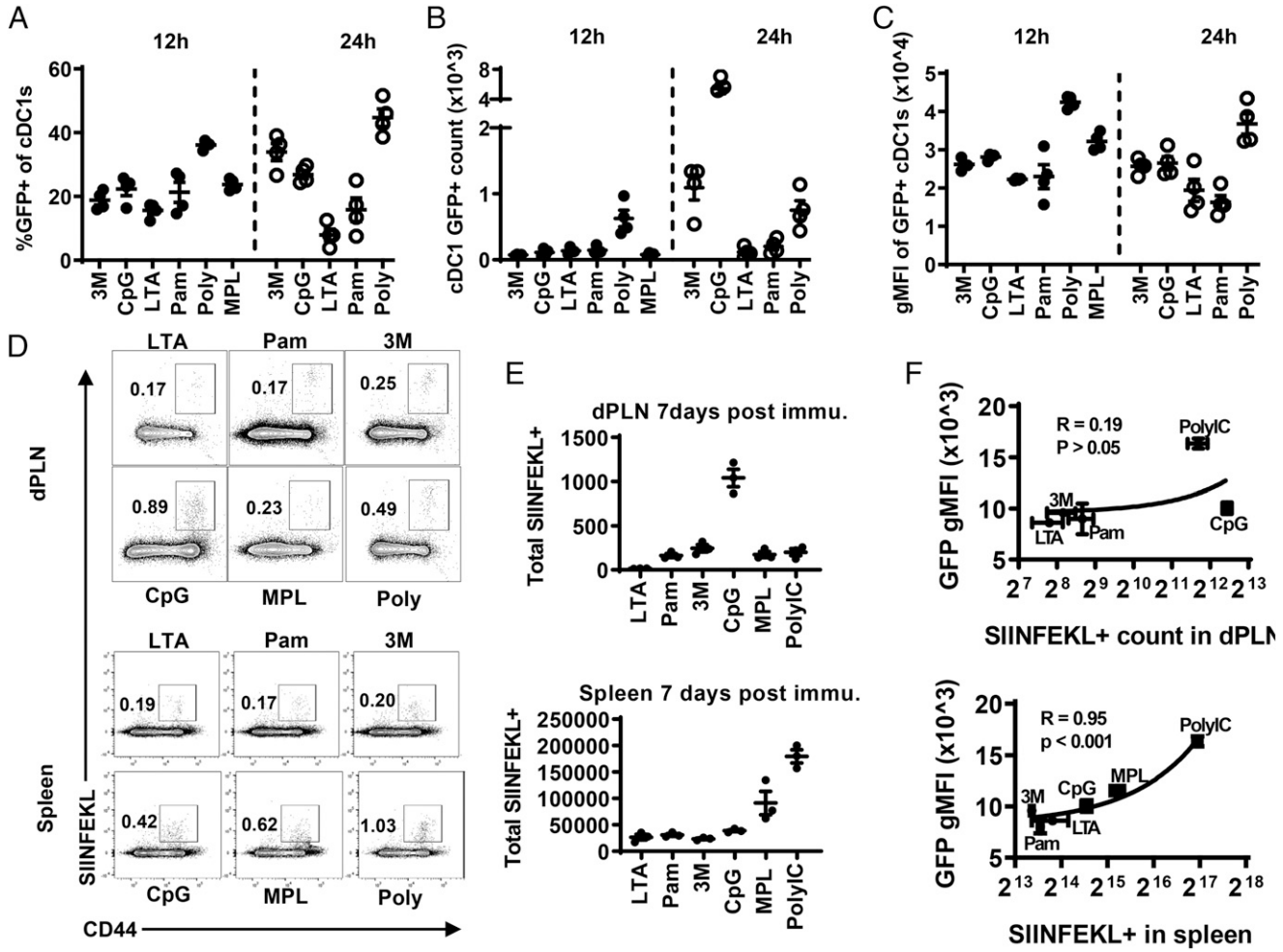

FIGURE 3. cDC1 IL-27p28 production at 12 h in the dPLN correlates with systemic T cell counts at 7 d. (**A**–**C**) IL-27p28-eGFP mice were immunized in the footpad with 10 μg indicated adjuvant and 25 μg OVA and dPLNs harvested 12 and 24 h later. Gated on cDC1s. (**D** and **E**) C57BL/6 mice were immunized in the footpad with 10 μg indicated adjuvant and 25 μg OVA, and dPLNs, blood, and spleens were harvested 7 d later. Gated on CD8s. (**F**) Linear regressions of correlations between data in (C) and (E). Data indicate means ± SEM, $n \geq 3$ mice per group, representative of two or more experiments.

to whether this relationship is affirming (3, 34) or opposing (35, 36). Unique to the data presented in this study, however, is our conclusion of the unexpected and unprecedented predictive value that the amount of IL-27p28 produced per cDC1 has on the magnitude of $CD8^+$ T cell memory.

In addition to pairing with EBI3 to form IL-27, IL-27p28 may also be secreted alone as a distinct cytokine known as IL-30 (37–39). As our reporter tracks only p28 expression, our results could conceivably identify a robust correlation between $CD8^+$ T cell memory formation and cDC1 IL-30, IL-27, or some combination of both. That being said, two lines of evidence point toward IL-27 as the more relevant cytokine. First, as mentioned above, the T cell response to subunit immunization is reliant on IL-27 signaling through T cell–expressed IL-27R (3). That is, the role of IL-27 in vaccine-elicited immunity can be observed under conditions of T cell–specific IL-27R deficiency. Although the specific receptor for IL-30 is as of yet undefined, it does not appear to be the IL-27R. Second, using an ELISA with capture specificity for IL-27p28 and detection of multiplexed bead array (that is, whole IL-27), high amounts of IL-27 are detected in the serum after vaccination and in the same time frame as cDC1 p28-eGFP expression (Supplemental Fig. 3F). These observations indicate that it is most likely IL-27, not IL-30, that correlates with and predicts the consequent $CD8^+$ T cell memory formation.

It is interesting that although some adjuvants augment the expansion of terminally differentiated effectors, this expansion does not seem to subtract from the MPEC/memory cell pool (Fig. 4). These conclusions are consistent with the model proposed by Chang and Reiner (40), whereby asymmetric segregation of fate-determining signaling and transcription factors generates daughter cells with different cell fates, ensuring the production of effector cells without compromising memory cell frequency. Additionally, it appears that the production of terminal effectors occurs after the initial immunization and T cell activation phase, perhaps related to the persisting inflammatory properties of the adjuvant used (41, 42). Although the total frequency of Ag-specific T cells is augmented by these adjuvants, this has no additional protective value against infectious challenge, perhaps related to the demonstrated negative consequences of a persisting Ag depot (15–17).

Although both resident and migratory cDC1s produce IL-27p28 in the draining node following peripheral immunization, only resident DC IL-27p28 production is predictive of the T cell response because this is the only population meaningfully present at 12 h after immunization. This was surprising given previous data by Jenkins and colleagues (29) showing the importance of the migratory DCs in maximizing the CD4 response to intradermal vaccination in the ear. It seems further distinct from the results of Heath and colleagues (43) in which migratory DCs were

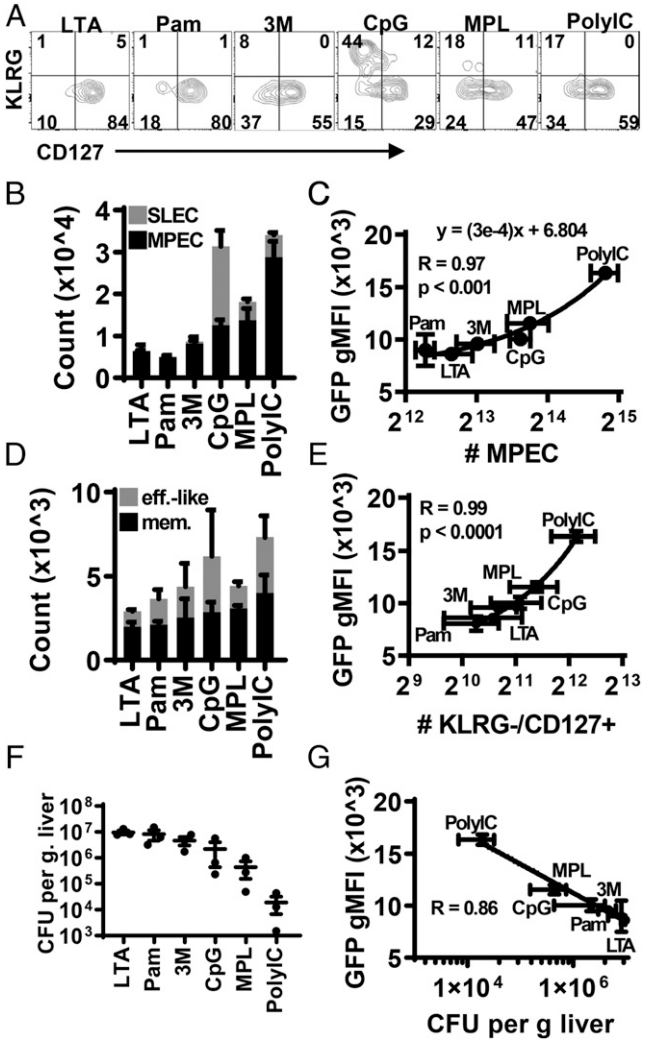

FIGURE 4. cDC1 IL-27p28 production at 12 h correlates with protection against infection at memory time points. (**A** and **B**) C57BL/6 mice were immunized in the footpad with 10 μg indicated adjuvant and 25 μg OVA, and dPLNs, blood, and spleens were harvested 10 d later (data from spleen shown). (**C**) Linear regression of correlation between data in Fig. 3C and in (B). (**D**) C57BL/6 mice were immunized in the footpad with 10 μg indicated adjuvant and 25 μg OVA, and spleens were harvested 50–80 d later. (**E**) Linear regression of correlation between data in Fig. 3C and in (D). (**F**) Memory-stage mice from (D) were challenged i.v. with 1.5×10^5 *L. monocytogenes*, and 4 d later, livers were harvested, homogenized, and plated in serial dilution on brain–heart infusion plates containing erythromycin. CFU of *L. monocytogenes* obtained per gram of liver. (**G**) Nonlinear regression of correlation between data in Fig. 3C and in (F). Data indicate means ± SEM, $n \geq 3$ mice per group, representative of two or more experiments.

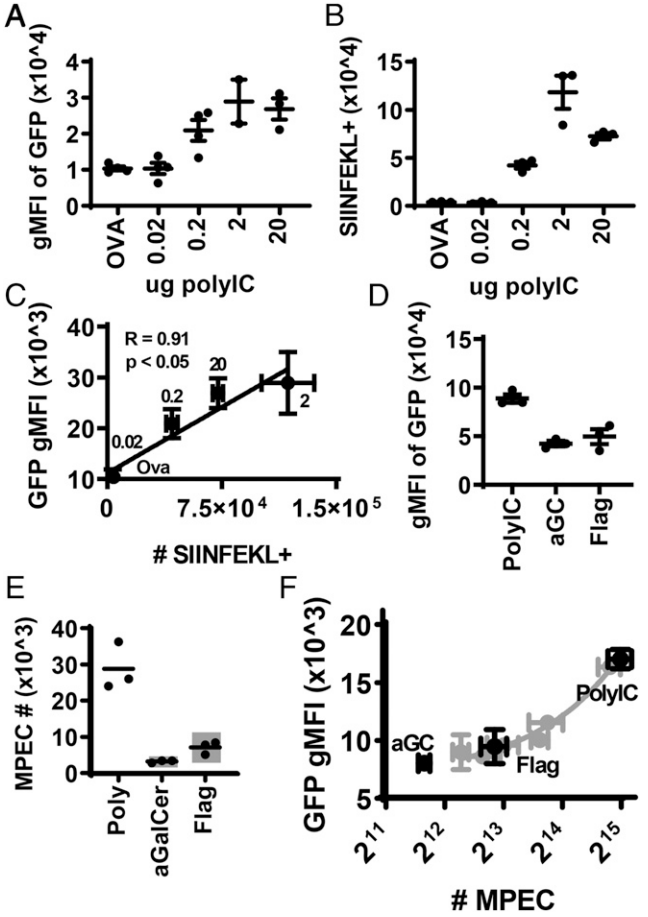

FIGURE 5. Early IL-27p28 production predicts the efficacy of novel adjuvants in generating protective T cell responses. (**A**) IL-27p28-eGFP mice were immunized in the footpad with an indicated amount of polyIC and 25 μg OVA, and dPLNs were harvested 12 h later. (**B**) C57BL/6 mice were immunized in the footpad with the indicated amount of polyIC and 25 μg OVA, and spleens were harvested 10 d later. (**C**) Linear regression of correlation between data in (A) and (B). (**D**) IL-27p28-eGFP mice were immunized in the footpad with 10 μg adjuvant and 25 μg OVA, and dPLNs were harvested 12 h later. (**E**) gMFIs for previously unexamined adjuvants from (D) were normalized against gMFIs obtained from polyIC-immunized mice harvested and analyzed simultaneously, and these adjusted gMFI levels were used to calculate the predicted T cell numbers (gray boxes) using the linear regression formula from Fig. 4C. Experimental values (black circles) were obtained by immunizing C57BL/6 mice in the footpad with 10 μg indicated adjuvant and 25 μg OVA and harvesting spleens 10 d later. (**F**) Overlay of values obtained in (D) and (E) with correlation plot from Fig. 4C. Data indicate means ± SEM, $n \geq 3$ mice per group, representative of two or more experiments.

critical for simulating naive T cells responding to HSV-1, whereas resident DCs were necessary for stimulating memory T cells. However, our data do not negate an important role for migratory cDC1s in our vaccine-elicited responses; they merely indicate that migratory cDC1 production of p28 is less predictive of downstream immunity than that produced by LN-resident cDC1s. Whether or not there is biology underlying this difference in predictive capacity specific to IL-27 signaling remains to be determined.

The magnitude of an immune response from local (s.c., intradermal, or i.m.) vaccine administration is often measured in the draining LN at the presumed peak (7–10 d) of the immune response. Our data indicate, however, that T cell number in the draining node at this time point correlates poorly with the overall magnitude of the T cell responses systemically. Given that $CD8^+$ T cells begin to migrate out from their initial site within a few days of Ag encounter, this is perhaps unsurprising, but it highlights the fact that caution should be used when using LN T cell numbers as a predictor of vaccine efficacy. Needing much more exploration is the role of activated T cell retention within the node, its relationship to the type of adjuvant used, and whether this retention within the node is beneficial or detrimental to downstream immunity.

It is intriguing to note that it was the cDC1 p28-eGFP gMFI, not the percentage of GFP^+, that best predicted downstream MPEC and memory formation. Thus, the amount of IL-27 produced per cDC1 appears to set the extent to which memory precursors, and ultimately memory T cells, are formed. This is at least consistent with the hypothesis that a T cell preferentially interacts

with p28-producing cDC1s and that this interaction is a determining factor in the magnitude of the ensuing response. Experiments using multiphoton microscopy are currently investigating the propensity cDC1 IL-27 production to influence the quantity/quality of T cell–DC interactions.

Finally, results from the titration of polyIC indicate that IL-27p28 production is not only a good biomarker for adjuvant efficacy but also for optimizing adjuvant dosing levels. Although much thought is often given to the appropriate dosing of Ag, less seems directed toward identifying the proper dosing of adjuvant, despite the growing recognition of the deleterious impact of excessive inflammation on tissue homeostasis and long-lived immune memory. Both CD4 and $CD8^+$ T cell responses are IL-27 dependent (3), so although we have only documented a predictive relationship between cDC1 expression of IL-27 and $CD8^+$ T cell elicitation, it seems likely that this will hold true for $CD4^+$ T cells as well. It is as of yet unclear to what degree IL-27 might predict humoral immunity. Because the majority of vaccines are directed toward the generation of Abs, it will be important to understand the role of IL-27 in B cell activation and whether any predictive correlations can be extracted from its interplay with IL-27–dependent $CD4^+$ T cell responses.

Acknowledgments

We thank the other members of the Kedl laboratory for helpful discussions throughout the preparation of the data and to Jared Klarquist for careful reading and editing of the manuscript.

Disclosures

The authors have no financial conflicts of interest.

References

1. Condotta, S. A., M. J. Richer, V. P. Badovinac, and J. T. Harty. 2012. Probing CD8 T cell responses with *Listeria monocytogenes* infection. *Adv. Immunol.* 113: 51–80.
2. Zehn, D., and E. J. Wherry. 2015. Immune memory and exhaustion: clinically relevant lessons from the LCMV model. *Adv. Exp. Med. Biol.* 850: 137–152.
3. Pennock, N. D., L. Gapin, and R. M. Kedl. 2014. IL-27 is required for shaping the magnitude, affinity distribution, and memory of T cells responding to subunit immunization. *Proc. Natl. Acad. Sci. USA* 111: 16472–16477.
4. Klarquist, J., A. Chitrakar, N. D. Pennock, A. M. Kilgore, T. Blain, C. Zheng, T. Danhorn, K. Walton, L. Jiang, J. Sun, et al. 2018. Clonal expansion of vaccine-elicited T cells is independent of aerobic glycolysis. *Sci. Immunol.* DOI: 10.1126/sciimmunol.aas9822.
5. Wehrens, E. J., K. A. Wong, A. Gupta, A. Khan, C. A. Benedict, and E. I. Zuniga. 2018. IL-27 regulates the number, function and cytotoxic program of antiviral CD4 T cells and promotes cytomegalovirus persistence. *PLoS One* 13: e0201249.
6. Wherry, E. J., T. C. Becker, D. Boone, M.-K. Kaja, A. Ma, and R. Ahmed. 2002. Homeostatic proliferation but not the generation of virus specific memory CD8 T cells is impaired in the absence of IL-15 or IL-15Ralpha. *Adv. Exp. Med. Biol.* 512: 165–175.
7. Becker, T. C., E. J. Wherry, D. Boone, K. Murali-Krishna, R. Antia, A. Ma, and R. Ahmed. 2002. Interleukin 15 is required for proliferative renewal of virus-specific memory CD8 T cells. *J. Exp. Med.* 195: 1541–1548.
8. Obar, J. J., S. G. Crist, E. K. Leung, and E. J. Usherwood. 2004. IL-15-independent proliferative renewal of memory CD8+ T cells in latent gammaherpesvirus infection. *J. Immunol.* 173: 2705–2714.
9. Holt, L. B. 1949. Quantitative studies in diphtheria prophylaxis; the primary response. *Br. J. Exp. Pathol.* 30: 289–297, pl.
10. Ehrenhofer, C., and J. P. Opdebeeck. 1995. The effects of continuous and intermittent delivery of antigens of Boophilus microplus on the development of murine antibodies. *Vet. Parasitol.* 59: 263–273.
11. Higaki, M., Y. Azechi, T. Takase, R. Igarashi, S. Nagahara, A. Sano, K. Fujioka, N. Nakagawa, C. Aizawa, and Y. Mizushima. 2001. Collagen minipellet as a controlled release delivery system for tetanus and diphtheria toxoid. *Vaccine* 19: 3091–3096.
12. Hu, J. K., J. C. Crampton, A. Cupo, T. Ketas, M. J. van Gils, K. Sliepen, S. W. de Taeye, D. Sok, G. Ozorowski, I. Deresa, et al. 2015. Murine antibody responses to cleaved soluble HIV-1 envelope trimers are highly restricted in specificity. *J. Virol.* 89: 10383–10398.
13. Kemp, J. M., M. Kajihara, S. Nagahara, A. Sano, M. Brandon, and S. Lofthouse. 2002. Continuous antigen delivery from controlled release implants induces significant and anamnestic immune responses. *Vaccine* 20: 1089–1098.
14. Tam, H. H., M. B. Melo, M. Kang, J. M. Pelet, V. M. Ruda, M. H. Foley, J. K. Hu, S. Kumari, J. Crampton, A. D. Baldeon, et al. 2016. Sustained antigen availability during germinal center initiation enhances antibody responses to vaccination. *Proc. Natl. Acad. Sci. USA* 113: E6639–E6648.
15. Assudani, D., H. I. Cho, N. DeVito, N. Bradley, and E. Celis. 2008. In vivo expansion, persistence, and function of peptide vaccine-induced CD8 T cells occur independently of CD4 T cells. *Cancer Res.* 68: 9892–9899.
16. Burchill, M. A., B. A. Tamburini, N. D. Pennock, J. T. White, J. S. Kurche, and R. M. Kedl. 2013. T cell vaccinology: exploring the known unknowns. *Vaccine* 31: 297–305.
17. Hailemichael, Y., Z. Dai, N. Jaffarzad, Y. Ye, M. A. Medina, X. F. Huang, S. M. Dorta-Estremera, N. R. Greeley, G. Nitti, W. Peng, et al. 2013. Persistent antigen at vaccination sites induces tumor-specific $CD8^+$ T cell sequestration, dysfunction and deletion. *Nat. Med.* 19: 465–472.
18. Kastelein, R. A., C. A. Hunter, and D. J. Cua. 2007. Discovery and biology of IL-23 and IL-27: related but functionally distinct regulators of inflammation. *Annu. Rev. Immunol.* 25: 221–242.
19. Pflanz, S., J. C. Timans, J. Cheung, R. Rosales, H. Kanzler, J. Gilbert, L. Hibbert, T. Churakova, M. Travis, E. Vaisberg, et al. 2002. IL-27, a heterodimeric cytokine composed of EBI3 and p28 protein, induces proliferation of naive CD4+ T cells. *Immunity* 16: 779–790.
20. Kilgore, A. M., S. Welsh, E. E. Cheney, A. Chitrakar, T. J. Blain, B. J. Kedl, C. A. Hunter, N. D. Pennock, and R. M. Kedl. 2018. IL-27p28 production by $XCR1^+$ dendritic cells and monocytes effectively predicts adjuvant-elicited $CD8^+$ T cell responses. *Immunohorizons* 2: 1–11.
21. Wegmann, F., A. E. Moghaddam, T. Schiffner, K. H. Gartlan, T. J. Powell, R. A. Russell, M. Baart, E. W. Carrow, and Q. J. Sattentau. 2015. The carbomer-lecithin adjuvant Adjuplex has potent immunoactivating properties and elicits protective adaptive immunity against influenza virus challenge in mice. *Clin. Vaccine Immunol.* 22: 1004–1012.
22. Scott, C. L., B. Soen, L. Martens, N. Skrypek, W. Saelens, J. Taminau, G. Blancke, G. Van Isterdael, D. Huylebroeck, J. Haigh, et al. 2016. The transcription factor Zeb2 regulates development of conventional and plasmacytoid DCs by repressing Id2. *J. Exp. Med.* 213: 897–911.
23. Dorner, B. G., M. B. Dorner, X. Zhou, C. Opitz, A. Mora, S. Güttler, A. Hutloff, H. W. Mages, K. Ranke, M. Schaefer, et al. 2009. Selective expression of the chemokine receptor XCR1 on cross-presenting dendritic cells determines cooperation with CD8+ T cells. *Immunity* 31: 823–833.
24. Kamath, A. T., J. Pooley, M. A. O'Keeffe, D. Vremec, Y. Zhan, A. M. Lew, A. D'Amico, L. Wu, D. F. Tough, and K. Shortman. 2000. The development, maturation, and turnover rate of mouse spleen dendritic cell populations. *J. Immunol.* 165: 6762–6770.
25. Kamath, A. T., S. Henri, F. Battye, D. F. Tough, and K. Shortman. 2002. Developmental kinetics and lifespan of dendritic cells in mouse lymphoid organs. *Blood* 100: 1734–1741.
26. Waskow, C., K. Liu, G. Darrasse-Jèze, P. Guermonprez, F. Ginhoux, M. Merad, T. Shengelia, K. Yao, and M. Nussenzweig. 2008. The receptor tyrosine kinase Flt3 is required for dendritic cell development in peripheral lymphoid tissues. *Nat. Immunol.* 9: 676–683.
27. Liu, K., C. Waskow, X. Liu, K. Yao, J. Hoh, and M. Nussenzweig. 2007. Origin of dendritic cells in peripheral lymphoid organs of mice. *Nat. Immunol.* 8: 578–583.
28. Alvarez, D., E. H. Vollmann, and U. H. von Andrian. 2008. Mechanisms and consequences of dendritic cell migration. *Immunity* 29: 325–342.
29. Itano, A. A., S. J. McSorley, R. L. Reinhardt, B. D. Ehst, E. Ingulli, A. Y. Rudensky, and M. K. Jenkins. 2003. Distinct dendritic cell populations sequentially present antigen to CD4 T cells and stimulate different aspects of cell-mediated immunity. *Immunity* 19: 47–57.
30. Wherry, E. J., V. Teichgräber, T. C. Becker, D. Masopust, S. M. Kaech, R. Antia, U. H. von Andrian, and R. Ahmed. 2003. Lineage relationship and protective immunity of memory CD8 T cell subsets. *Nat. Immunol.* 4: 225–234.
31. Gorden, K. B., K. S. Gorski, S. J. Gibson, R. M. Kedl, W. C. Kieper, X. Qiu, M. A. Tomai, S. S. Alkan, and J. P. Vasilakos. 2005. Synthetic TLR agonists reveal functional differences between human TLR7 and TLR8. *J. Immunol.* 174: 1259–1268.
32. Hayashi, F., K. D. Smith, A. Ozinsky, T. R. Hawn, E. C. Yi, D. R. Goodlett, J. K. Eng, S. Akira, D. M. Underhill, and A. Aderem. 2001. The innate immune response to bacterial flagellin is mediated by toll-like receptor 5. *Nature* 410: 1099–1103.
33. Matsuda, J. L., O. V. Naidenko, L. Gapin, T. Nakayama, M. Taniguchi, C. R. Wang, Y. Koezuka, and M. Kronenberg. 2000. Tracking the response of natural killer T cells to a glycolipid antigen using CD1d tetramers. *J. Exp. Med.* 192: 741–754.
34. Huang, Z., J. Zak, I. Pratumchai, N. Shaabani, V. F. Vartabedian, N. Nguyen, T. Wu, C. Xiao, and J. R. Teijaro. 2019. IL-27 promotes the expansion of self-renewing $CD8^+$ T cells in persistent viral infection. *J. Exp. Med.* 216: 1791–1808.
35. Chihara, N., A. Madi, T. Kondo, H. Zhang, N. Acharya, M. Singer, J. Nyman, N. D. Marjanovic, M. S. Kowalczyk, C. Wang, et al. 2018. Induction and transcriptional regulation of the co-inhibitory gene module in T cells. *Nature* 558: 454–459.
36. Gwyer Findlay, E., A. Villegas-Mendez, N. O'Regan, J. B. de Souza, L.-M. Grady, C. J. Saris, E. M. Riley, and K. N. Couper. 2014. IL-27 receptor signaling regulates memory CD4+ T cell populations and suppresses rapid inflammatory responses during secondary malaria infection. *Infect. Immun.* 82: 10–20.

37. Dibra, D., J. Cutrera, X. Xia, B. Kallakury, L. Mishra, and S. Li. 2012. Interleukin-30: a novel antiinflammatory cytokine candidate for prevention and treatment of inflammatory cytokine-induced liver injury. *Hepatology* 55: 1204–1214.
38. Zhang, S., R. Liang, W. Luo, C. Liu, X. Wu, Y. Gao, J. Hao, G. Cao, X. Chen, J. Wei, et al. 2013. High susceptibility to liver injury in IL-27 p28 conditional knockout mice involves intrinsic interferon-γ dysregulation of CD4+ T cells. *Hepatology* 57: 1620–1631.
39. Mitra, A., A. Satelli, J. Yan, X. Xueqing, M. Gagea, C. A. Hunter, L. Mishra, and S. Li. 2014. IL-30 (IL27p28) attenuates liver fibrosis through inducing NKG2D-rae1 interaction between NKT and activated hepatic stellate cells in mice. *Hepatology* 60: 2027–2039.
40. Chang, J. T., and S. L. Reiner. 2008. Asymmetric division and stem cell renewal without a permanent niche: lessons from lymphocytes. *Cold Spring Harb. Symp. Quant. Biol.* 73: 73–79.
41. Badovinac, V. P., K. A. Messingham, A. Jabbari, J. S. Haring, and J. T. Harty. 2005. Accelerated CD8+ T-cell memory and prime-boost response after dendritic-cell vaccination. *Nat. Med.* 11: 748–756.
42. Danilo, M., V. Chennupati, J. G. Silva, S. Siegert, and W. Held. 2018. Suppression of Tcf1 by inflammatory cytokines facilitates effector CD8 T cell differentiation. *Cell Rep.* 22: 2107–2117.
43. Belz, G. T., S. Bedoui, F. Kupresanin, F. R. Carbone, and W. R. Heath. 2007. Minimal activation of memory CD8+ T cell by tissue-derived dendritic cells favors the stimulation of naive CD8+ T cells. *Nat. Immunol.* 8: 1060–1066.